UNKNOWN MULTIPLE NARROW-BAND DISTURBANCE REJECTION IN HARD DISK DRIVES–AN ADAPTIVE NOTCH FILTER AND PERFECT DISTURBANCE OBSERVER APPROACH

Xu Chen
Department of Mechanical Engineering
University of California, Berkeley
Berkeley, California 94720
Email: maxchen@me.berkeley.edu

Masayoshi Tomizuka
Department of Mechanical Engineering
University of California, Berkeley
Berkeley, California 94720
Email: tomizuka@me.berkeley.edu

ABSTRACT

In this paper, an adaptive control scheme is developed to reject unknown multiple narrow-band disturbances in a hard disk drive. An adaptive notch filter is developed to efficiently estimate the frequencies of the disturbance. Based on the correctly estimated parameters, a disturbance observer with a newly designed multiple band-pass filter is constructed to achieve asymptotic perfect rejection of the disturbance. Evaluation of the control scheme is performed on a benchmark problem for HDD track following.

1 INTRODUCTION

The track following control in a hard disk drive (HDD) system aims at precisely regulating the read/write head on the data track and reducing the Track Mis-Registration (TMR). One important source of TMR is the vibration/flutter of disks at their resonant frequencies. This behavior is driven by the turbulent air flow within the hard disk assembly, and creates the so-called non-repeatable multiple narrow-band disturbances [1–3], whose energy is highly concentrated at several unknown frequencies. These disturbances differ from track to track and disk to disk in nature, and may appear at frequencies higher than the open loop servo bandwidth [1,2]. The above characteristics of narrow-band disturbances lead to the difficulty of rejecting them using traditional feedback control methods. With the rapid growth in HDD's storage density, compensation of the non-repeatable multiple narrow-band disturbances is becoming more and more an important issue.

Improving the mechanical design can help to reduce the narrow-band disturbances but will significantly increase the product cost. Investigation of this problem in the community of systems and controls has therefore been popular. For example, Zheng and Tomizuka [4–6] suggested direct and indirect adaptive disturbance observer (DOB) schemes to estimate and cancel the disturbance; Kim et al. [7] proposed a parallel add-on peak filter to shape the open loop frequency response; Landau [8] used Youla-Kucera parametrization to achieve adaptive narrow-band disturbance rejection on an active suspension. These previous methods have been focusing on rejecting disturbance with one narrow-band. Yet, the field of multiple narrow-band disturbance rejection was seldom entered before.

This paper focuses on developing an adaptive control scheme that compensates *any* number of unknown narrow-band disturbances. The main techniques proposed are the minimal parameter adaptive notch filter (ANF) for frequency identification and the disturbance observer (DOB) for disturbance rejection. The minimal parameter ANF was developed in the signal processing community, rooted back to [9], refined first in [10] and then in [11]. It has the advantage of high computational efficiency, good numerical robustness, and fast convergence. This paper proposes a computationally simplified version of [11], to fit the algorithm for our controller structure. The accurately identified frequencies are then applied to construct a new type of DOB, which can asymptotically achieve perfect narrow-band disturbance rejection. Advantages of the proposed algorithm are: it inherits the excellent properties of the minimal parameter ANF in the frequency identification; it is an add-on compensator and can be simply integrated to the existing baseline controller structure; it rejects the narrow-band disturbance with minor influence to the system sensitivity function at other frequencies; it can achieve asymptotic perfect disturbance rejection.

The remainder of this paper is organized as follows. Section 2 formally defines the problem. The proposed DOB structure, and the design of a multiple narrow band-pass Q-filter are presented in Section 3. Section 4 provides the adaptive ANF algorithm for Q-filter parameter identification. The efficacy of the proposed method is provided in Section 5, with an example of rejecting two narrow-band disturbances. Section 6 concludes the paper.

2 PROBLEM DEFINITION

Figure 1 shows the baseline feedback control loop for HDD track following and the proposed compensation scheme to reject the multiple narrow-band disturbances. The full-order plant model $G_p\left(z^{-1}\right)$ contains the dynamics of the HDD servo system including the power amplifier, the voice-coil motor, and the actuator mechanics. Throughout the paper we use the well formulated open-source HDD benchmark simulation package [12] as a demonstration tool. The dashed line in Fig. 2 shows the frequency response of $G_p\left(z^{-1}\right)$, which is a fourteenth-order transfer function with several high frequency resonances. The low order nominal plant model $z^{-m}G_n\left(z^{-1}\right)$ matches the low-frequency dynamics of $G_p\left(z^{-1}\right)$ up to about 2000 Hz, as shown in Fig. 2. The baseline feedback controller $C_{FB}\left(z^{-1}\right)$ is a commonly used PID controller cascaded with three notch filters. Figure 3 shows the frequency response of the open loop system $C_{FB}\left(z^{-1}\right)G_p\left(z^{-1}\right)$, which has a gain margin of 5.45 dB, a phase margin of 38.2 deg, and an open loop servo bandwidth of 1.19 kHz.

The signals $r(k)$, $d(k)$, $u(k)$, and $n(k)$, are respectively the reference, the input disturbance, the control input, and the output disturbance. PES is the position error signal. The multiple narrow-band disturbances of interest are assumed to be contained in $d(k)$, and have unknown frequencies between 300 Hz and 2000 Hz [1,2].

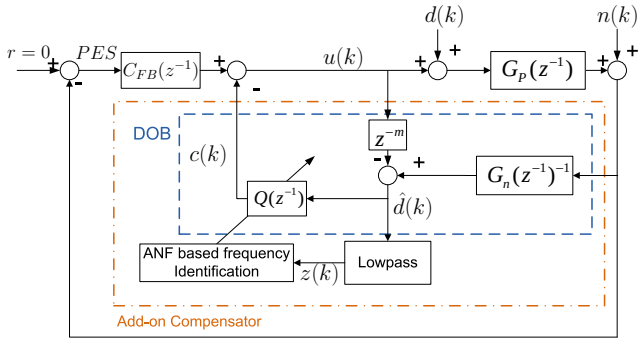

Figure 1. Structure of the proposed scheme for multiple narrow-band disturbance rejection.

We observe from Fig. 3, that the general baseline open loop system has a decreasing high gain in the low frequency region,

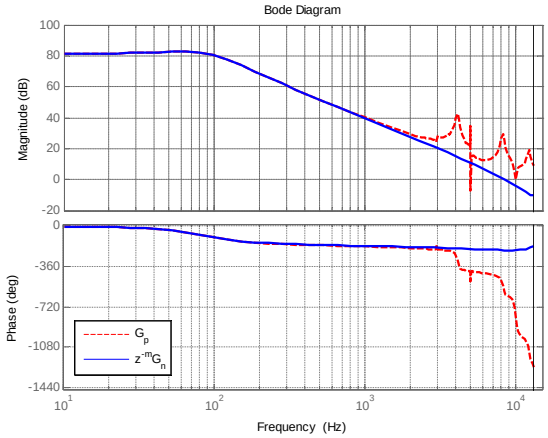

Figure 2. Frequency responses of the full order plant and its nominal model.

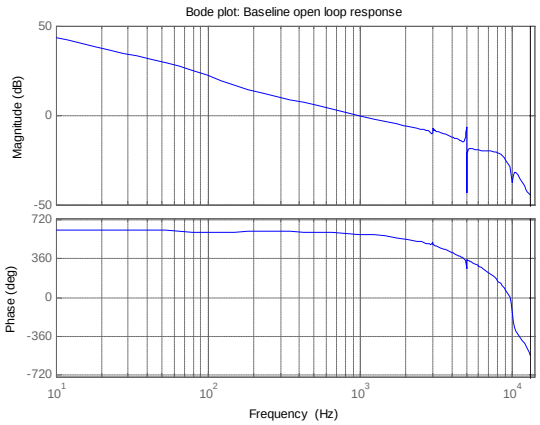

Figure 3. Frequency response of the open loop system with the baseline controller $C_{FB}\left(z^{-1}\right)$.

which indicates that the closed loop system suppresses low frequency disturbance but has less and less attenuation capacity as the frequency increases. When special attenuation is needed at several narrow frequency regions (say around 500 Hz and 1000 Hz), the baseline controller would fail to maintain the desired servo performance. In this paper, we aim at providing a solution to this important problem.

3 DOB FOR MULTIPLE NARROW-BAND DISTURBANCE REJECTION

The proposed control scheme for multiple narrow-band disturbance rejection is summarized in the dash-dotted box in Fig. 1. The add-on compensator is a disturbance observer (DOB) [13] with a specially designed adaptive Q-filter $Q\left(z^{-1}\right)$. As the name of DOB suggests, the multiple narrow-band disturbance is 'observed' by the controller, and fed back to cancel itself. To see this point, notice first that the signal $\hat{d}(k)$ is expressed by, in the

operator notation,

$$\hat{d}(k) = G_n(z^{-1})^{-1}[G_p(z^{-1})(u(k)+d(k))+n(k)] - z^{-m}u(k) \tag{1}$$

A stable inverse model $G_n\left(z^{-1}\right)^{-1}$ is needed in the above signal processing. If $G_n\left(z^{-1}\right)$ has minimal phase, its inverse can directly be assigned, if not, stable inversion techniques such as the ZPET method [14] should be applied.

Noting that $G_n\left(z^{-1}\right)^{-1} = z^{-m}\left(z^{-m}G_n\left(z^{-1}\right)\right)^{-1}$, we can transform Eq. (1) to

$$\begin{aligned}
&\hat{d}(k)\\
=&z^{-m}\left\{\left(z^{-m}G_n\left(z^{-1}\right)\right)^{-1}G_p\left(z^{-1}\right)u(k) - u(k)\right\}\\
&+z^{-m}\left(z^{-m}G_n\left(z^{-1}\right)\right)^{-1}G_p\left(z^{-1}\right)d(k)\\
&+G_n\left(z^{-1}\right)^{-1}n(k).
\end{aligned} \tag{2}$$

Notice that $z^{-m}G_n\left(z^{-1}\right) \approx G_p\left(z^{-1}\right)$ under 2000 Hz, which gives $\left[\left(z^{-m}G_n\left(z^{-1}\right)\right)^{-1}G_p\left(z^{-1}\right)\right]u(k) - u(k) \approx 0$. If in addition the output disturbance $n(k)$ is small, then Eq. (2) becomes

$$\hat{d}(k) \approx z^{-m}d(k) = d(k-m). \tag{3}$$

The above equation implies that $\hat{d}(k)$ is a good estimate of $d(k)$, i.e., the disturbance is well 'observed' by DOB.

In reality, the influence of $n(k)$ and other noise can not be omitted. To compensate only the narrow-band disturbance without influencing other components in $d(k)$, it is proposed to pass $\hat{d}(k)$ through a multiple band-pass filter $Q\left(z^{-1}\right)$, whose pass-bands are sharply located at the narrow-band frequencies. The compensation signal $c(k)$ formed by filtering $\hat{d}(k)$ through $Q\left(z^{-1}\right)$, therefore contains only the multiple narrow-band disturbance. Adding the negative of $c(k)$ to the control input, we achieve the compensation.

3.1 Q-filter Design for Perfect Disturbance Rejection

Assume that the multiple narrow-band frequencies are at $\Omega_1, \ldots, \Omega_n$ (in Hz). Estimation of these frequencies will be discussed in the next section. In this section, we present the structural design of $Q\left(z^{-1}\right)$, and assume Ω_i's are known.

To have sharp pass-bands at Ω_i's, poles of $Q\left(z^{-1}\right)$ need to be located close to these frequencies. The second constraint on $Q\left(z^{-1}\right)$ comes from Eq. (3), that the estimated disturbance $\hat{d}(k)$ is a m-step delayed version of the true signal $d(k)$. This translates to the need on $Q\left(z^{-1}\right)$ to be able to provide a m-step forward action to $\hat{d}(k)$.

Suppose the basis Q-filter for *single* narrow-band disturbance rejection has the form $Q_0\left(z^{-1}\right) = N_Q\left(z^{-1}\right)/D_Q\left(z^{-1}\right)$, where $N_Q\left(z^{-1}\right)$ and $D_Q\left(z^{-1}\right)$ are polynomials of z^{-1}. Using the results in the last subsection, that $\hat{d}(k) \approx d(k-m)$ and $c(k) = Q\left(z^{-1}\right)\hat{d}(k)$, we have

$$\begin{aligned}
d(k) - c(k) &\approx \left(1 - z^{-m}Q\left(z^{-1}\right)\right)d(k)\\
&= \frac{D_Q\left(z^{-1}\right) - z^{-m}N_Q\left(z^{-1}\right)}{D_Q\left(z^{-1}\right)}d(k).
\end{aligned} \tag{4}$$

When $d(k)$ is a narrow-band sinusoidal signal with frequency Ω_o (in Hz) and sampling time T_s (in sec), by direct expansion, one can show that $\left(1 - 2\cos(\omega_o)z^{-1} + z^{-2}\right)d(k) = 0$[1], where $\omega_o = 2\pi\Omega_o T_s$. Therefore, if $D_Q\left(z^{-1}\right)$ is stable in Eq. (4), and

$$D_Q(z^{-1}) - z^{-m}N_Q(z^{-1}) = J(z^{-1})\left[1 - 2\cos(\omega_o)z^{-1} + z^{-2}\right], \tag{5}$$

where $J\left(z^{-1}\right)$ is a polynomial of z^{-1}, we can achieve asymptotic perfect disturbance rejection, i.e.,

$$\lim_{k\to\infty}(d(k) - c(k)) = 0. \tag{6}$$

In our nominal model, $m = 1$. Assign $J\left(z^{-1}\right) = 1$, and let $D_Q\left(z^{-1}\right)$ be given by

$$D_Q\left(z^{-1}\right) = 1 - 2\alpha\cos(\omega_0)z^{-1} + \alpha^2 z^{-2}, \tag{7}$$

where the shaping coefficient α is a real number smaller than but close to 1, such that $Q\left(z^{-1}\right)$ is stable and has two poles $\alpha e^{\pm j\omega_0}$ at the narrow-band frequency.

Substituting Eq. (7) to Eq. (5), and applying the method of undetermined coefficients, we get

$$N_Q\left(z^{-1}\right) = 2(1-\alpha)\cos(\omega_0) + \left(\alpha^2 - 1\right)z^{-1}. \tag{8}$$

Introduce now the shorthand notation $\theta_0 = \cos(\omega_0)$. The ideal Q-filter for *single* narrow-band disturbance rejection is thus given by

$$Q_0\left(z^{-1}\right) = \frac{2(1-\alpha)\theta_0 + \left(\alpha^2 - 1\right)z^{-1}}{1 - 2\alpha\theta_0 z^{-1} + \alpha^2 z^{-2}}. \tag{9}$$

When $d(k)$ contains n narrow-band components, the above equation can be extended to

$$Q\left(z^{-1}\right) = \sum_{i=1}^{n}\frac{2(1-\alpha_i)\theta_i + \left(\alpha_i^2 - 1\right)z^{-1}}{1 - 2\alpha_i\theta_i z^{-1} + \alpha_i^2 z^{-2}}, \tag{10}$$

[1] $1/\left(1 - 2\cos(\omega_o)z^{-1} + z^{-2}\right)$ is also known as the internal model of the narrow band disturbance $d(k)$.

Figure 4 shows the frequency response of the above $Q\left(z^{-1}\right)$ with $\alpha_1 = \alpha_2 = 0.998$, $T_s = 3.788 \times 10^{-5}$ sec, $\theta_1 = \cos\left(2\pi \times 500 T_s\right)$, and $\theta_2 = \cos\left(2\pi \times 1200 T_s\right)$. Notice that at the central frequencies, the magnitude and the phase of $Q\left(z^{-1}\right)$ are 1 (0 dB) and 0 deg, respectively. Therefore, passing a broad band disturbance $\hat{d}(k)$ through $Q\left(z^{-1}\right)$, one filters out other components and gets only the multiple narrow-band signals at 500 Hz and 1200 Hz.

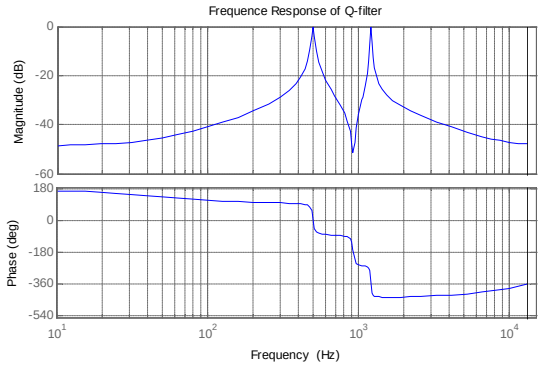

Figure 4. Frequency response of a Q-filter with two narrow pass-bands.

The error rejection property of a control system is commonly evaluated by its sensitivity function $S\left(z^{-1}\right)$, which is the transfer function from the output disturbance to the feedback error signal. Figure 5 shows the frequency response of $S\left(z^{-1}\right)$ for the proposed overall control structure when $Q\left(z^{-1}\right)$ is fixed. With the add-on compensation scheme, PES at 500 Hz and 1200 Hz can get greatly attenuated, due to the deep notches in the magnitude response at the corresponding frequencies, while the influence to the sensitivity at other frequencies is neglectable.

Stability of DOB (see [15, 16]) requires the nominal model $z^{-m}G_n\left(z^{-1}\right)$ to have no zeros outside the unit circle and that

$$\left|Q\left(e^{j\omega}\right)\right| < \frac{1}{\left|\Delta\left(e^{j\omega}\right)\right|} \quad \forall\omega, \tag{11}$$

where $\Delta(z^{-1}) = \left[G_p(z^{-1}) - z^{-m}G_n(z^{-1})\right]/z^{-m}G_n(z^{-1})$ represents the multiplicative model mismatch. Plotting the magnitude responses of $1/\Delta\left(z^{-1}\right)$ and $Q\left(z^{-1}\right)$ in Fig. 6, we see that the proposed DOB is stable as long as the narrow-band frequency is less than 3000 Hz.

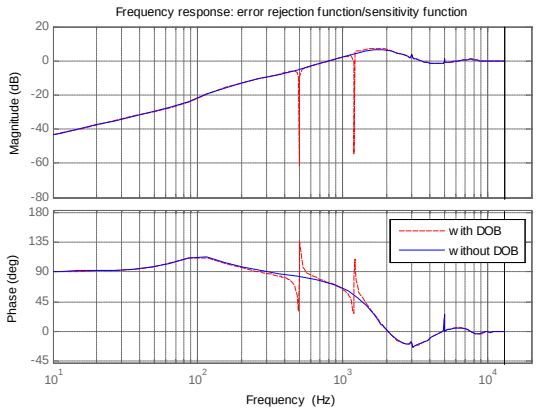

Figure 5. Frequency response of the closed loop sensitivity function.

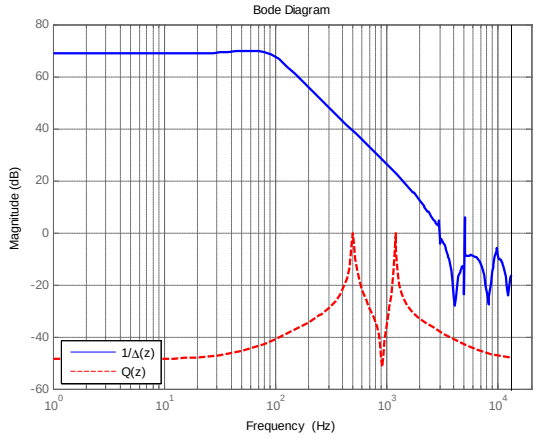

Figure 6. Magnitude responses of $1/\Delta\left(z^{-1}\right)$ and $Q\left(z^{-1}\right)$.

4 ADAPTIVE NOTCH FILTER FOR FREQUENCY IDENTIFICATION

The proposed Q-filter design requires knowledge of the frequency information $\theta_i = \cos\left(2\pi\Omega_i T_s\right)$, which is not priori available. In this section, we apply an adaptive notch filter (ANF) algorithm to estimate these quantities. As has been discussed before, $\hat{d}(k)$ contains the multiple narrow-band disturbance as well as other noise components. A low-pass filter is thus first constructed to filtered out the components in $\hat{d}(k)$ that are out of interest. The filtered signal $z(k)$ is finally a multiple narrow-band signal with small noise-signal ratio, and can be identified using the parameter estimation scheme in this section.

4.1 Theory

The intuition of the ANF algorithm comes from the fact that energy of the narrow-band disturbance $z(k)$ is highly concentrated at several frequencies $\Omega = [\Omega_1, \ldots, \Omega_n]^T$ (in Hz). If one constructs a notch filter $H\left(z^{-1}\right)$ with multiple center frequencies at $[\Omega_1, \ldots, \Omega_n]^T$, and passes $z(k)$ through $H\left(z^{-1}\right)$, the output $e^o(k)$ should have the least energy.

Introduce the normalized frequency $\omega_i = 2\pi\Omega_i T_s$ (in radians). The transfer function of a qualifying notch filter [11] is

given by

$$H\left(z^{-1}\right)=\prod_{i=1}^{n}H_o\left(\omega_i,z^{-1}\right), \tag{12}$$

where

$$H_o\left(\omega_i,z^{-1}\right)=\frac{1-2\beta z^{-1}\cos\omega_i+\beta^2 z^{-2}}{1-2\alpha z^{-1}\cos\omega_i+\alpha^2 z^{-2}}. \tag{13}$$

$H_o\left(\omega_i,z^{-1}\right)$ has two poles at $\alpha e^{\pm j\omega_i}$ and two zeros at $\beta e^{\pm j\omega_i}$. With the shaping coefficients β chosen close to 1, and $\alpha<\beta<1$, the filter will have a strong attenuation to the input signal at frequency ω_i.

To find the unknown $\omega_i's$, an adaptive algorithm is necessary. Considering the numerator and the denominator of $H\left(z^{-1}\right)$ as two entire sections[2] and estimating their coefficients, Nehorai developed the algorithm in [9]. Applying the cascaded series of second-order sections as shown in Eq. (12), and updating directly ω_i gave rise to [10], which was later refined in [11]. The above algorithms identify only n parameters, which is the minimum possible number for n narrow-band components. The main advantage of [11] over [9] is that cascaded filter structures are numerically more efficient and stable when the filter order is high [17].

We notice, however, from the control aspect of view, that the value of ω_i is not directly needed ($\cos\omega_i$ is the term really implemented in the controller). To directly estimate ω_i, [10] and [11] needed to calculate trigonometric functions within each iteration, which can be an expensive task in HDD servo control, since the microprocessor has limited ability in these computations. To localize the ANF method for HDD control, we introduce $\theta_i=\cos(\omega_i)$, and modify the algorithm in [11] as follows:

In Eq. (13), let

$$A_o\left(\theta_i,\gamma z^{-1}\right)=1-2\gamma z^{-1}\theta_i+\gamma^2 z^{-2},\ \gamma=\alpha,\beta, \tag{14}$$

and introduce the unknown parameter vector $\theta=[\theta_1,\theta_2\cdots\theta_n]^T$, Eq. (12) becomes

$$H\left(\theta,z^{-1}\right)=\prod_{i=1}^{n}H_o\left(\theta_i,z^{-1}\right)=\prod_{i=1}^{n}\frac{A_o\left(\theta_i,\beta z^{-1}\right)}{A_o\left(\theta_i,\alpha z^{-1}\right)}, \tag{15}$$

where we used the notation $H\left(\theta,z^{-1}\right)$ to emphasize that this is a transfer function with unknown parameter θ. The objective of ANF design is to find the best parameter estimate, such that the following cost function is minimized

$$V_k=\sum_{j=1}^{k}\frac{1}{2}\left[e^o(j)\right]^2, \tag{16}$$

[2] i.e., applying the digital filter in its direct-form structure.

where $e^0(k)=H\left(\theta,z^{-1}\right)z(k)$ is the output error.

The transfer function $H\left(\theta,z^{-1}\right)$ is nonlinear in θ. To find the best estimation, the celebrated Gauss-Newton Recursive Prediction Error Method (RPEM) (chapter 11 in [18]) suggests to apply the following iterative formulas

$$\hat{\theta}(k)=\hat{\theta}(k-1)+\frac{F(k-1)\psi(k-1)e^o(k)}{\lambda(k)+\psi^T(k-1)F(k-1)\psi(k-1)}, \tag{17}$$

$$F(k)=\frac{1}{\lambda(k)}\left[F(k-1)-\frac{F(k-1)\psi(k-1)\psi^T(k-1)F(k-1)}{\lambda(k)+\psi^T(k-1)F(k-1)\psi(k-1)}\right], \tag{18}$$

where $\psi(k-1)=[\psi_1(k-1),\ldots,\psi_n(k-1)]^T$, $\psi_i(k-1)=-\partial e^o(k)/\partial\hat{\theta}_i(k-1)$, and $\lambda(k)$ is the forgetting factor.

The above modified algorithm has several nice properties:

1. stability of the Gauss-Newton RPEM is guaranteed if $H(\hat{\theta}(k),z^{-1})$ is stable during the adaptation [18], which can be easily checked by monitoring if $|\hat{\theta}_i(k)|<1$, due to our cascaded construction of Eq. (15).
2. $\hat{\theta}(k)$ unbiasedly converges to a local minimum [18].
3. it inherits most of the advantages of [9,11], such as fast convergence, computational efficiency, and numerical robustness. Moreover, it does not require computing sine and cosine functions.

4.2 Algorithm

Similar to [11], to obtain first $e^0(k)=H\left(\theta,z^{-1}\right)z(k)$, we introduce

$$x_j(k)=\prod_{i=1}^{j}H_0\left(\theta_i,z^{-1}\right)z(k), \tag{19}$$

from which we have

$$x_j(k)=\frac{1-2\beta\theta_i z^{-1}+\beta^2 z^{-2}}{1-2\alpha\theta_i z^{-1}+\alpha^2 z^{-2}}x_{j-1}(k), \tag{20}$$

i.e., in the state-space representation

$$Z_i(k+1)=\left[\begin{array}{c|c}2\alpha\theta_i & -\alpha^2\\ \hline 1 & 0\end{array}\right]Z_i(k)+\left[\begin{array}{c}1\\ \hline 0\end{array}\right]x_{i-1}(k), \tag{21}$$

$$x_i(k)=[2(\alpha-\beta)\theta_i,\beta^2-\alpha^2]Z_i(k)+x_{i-1}(k). \tag{22}$$

We can then iteratively get $e^0(k)$, with $e^o(k)=x_n(k)$ and $x_0(k)=z(k)$.

To get $\psi_i(k-1) = -\partial e^o(k)/\partial\hat{\theta}_i(k-1)$, we notice that

$$\begin{aligned}\frac{\partial e^o(k)}{\partial\hat{\theta}_i(k-1)} &= \frac{\partial H\left(\hat{\theta}_i(k-1), z^{-1}\right) z(k)}{\partial\hat{\theta}_i(k-1)} \\ &= \frac{\partial H_o\left(\hat{\theta}_i(k-1), z^{-1}\right)}{\partial\hat{\theta}_i(k-1)} \prod_{j\neq i} H_o\left(\hat{\theta}_j(k-1), z^{-1}\right) z(k) \\ &= \frac{\partial H_o\left(\hat{\theta}_i(k-1), z^{-1}\right)}{\partial\hat{\theta}_i(k-1)} H_o^{-1}\left(\hat{\theta}_i(k-1), z^{-1}\right) e^o(k). \end{aligned} \quad (23)$$

Using Eq. (14) and Eq. (15), we get

$$\begin{aligned}\frac{\partial H_o\left(\theta_i, z^{-1}\right)}{\partial\theta_i} = &\frac{\frac{\partial A_o\left(\theta_i,\beta z^{-1}\right)}{\partial\theta_i} A_o\left(\theta_i,\alpha z^{-1}\right)}{A_o^2\left(\theta_i,\alpha z^{-1}\right)} \\ &- \frac{A_o\left(\theta_i,\beta z^{-1}\right)\frac{\partial A_o\left(\theta_i,\alpha z^{-1}\right)}{\partial\theta_i}}{A_o^2\left(\theta_i,\alpha z^{-1}\right)}, \end{aligned} \quad (24)$$

where $\partial A_o\left(\theta_i,\gamma z^{-1}\right)/\partial\theta_i = -2\gamma z^{-1}$, $\gamma = \alpha,\beta$. Substituting the above back to Eq. (23), and changing θ_i to its estimated value $\hat{\theta}_i(k-1)$, we arrive at the following simple formula:

$$\psi_i(k-1) = 2\left[e_{F_i}(\beta,k) - e_{F_i}(\alpha,k)\right], \quad (25)$$

where $e_{F_i}(\gamma,k) = \gamma z^{-1}/A_o\left(\hat{\theta}_i(k-1),\gamma z^{-1}\right) e^o(k)$, $\gamma = \alpha,\beta$, which can again be calculated using a state-space realization

$$W_i(\gamma,k+1) = \left[\begin{array}{c|c} 2\gamma\hat{\theta}_i(k) & -\gamma^2 \\ \hline 1 & 0 \end{array}\right] W_i(\gamma,k) + \left[\begin{array}{c} 1 \\ \hline 0 \end{array}\right] e^o(k), \quad (26)$$

$$e_{F_i}(\gamma,k) = \left[\gamma,\ 0\right] W_i(\gamma,k). \quad (27)$$

We notice that the above result has a similar structure with that in [11], but does not require to calculate sine or cosine functions. Analogous to [11], the recursive parameter estimation is finally summarized as follows:

Initialization: $\alpha_o = 0.8$, $\alpha_{end} = 0.995$, $\alpha_{rate} = 0.99$,[3] $\beta = 0.9999$, $Z_i(0) = W_i(\gamma,0) = 0$, $F(0) \approx 100/E\left[e^o\right]^2 \cdot I$, $\hat{\theta}(0) =$ initial guess of the parameters, $\lambda(0) = \lambda_0$, $\lambda(\infty) = \lambda_{end}$, $\lambda_{rate} = 0.99$.

Main loop: for $k = 1,2,\ldots$

step 1, prediction error computation: for $i = 1:n$

$$x_i(k) = [2(\alpha-\beta)\hat{\theta}_i(k-1), \beta^2-\alpha^2] Z_i(k) + x_{i-1}(k), \quad (28)$$

with $x_0(k) = z(k)$ and $e^o(k) = x_n(k)$.

[3] α is designed to increase exponentially from α_o to α_∞, at the rate of α_{rate}, such that the notches get sharper and sharper to better capture the narrow-band frequencies.

step 2, regressor vector computation: for $i = 1:n$

$$e_{F_i}(\gamma,k) = \left[\gamma,\ 0\right] W_i(\gamma,k),\ \gamma = \alpha,\beta, \quad (29)$$

$$\psi_i(k-1) = 2\left(e_{F_i}(\beta,k) - e_{F_i}(\alpha,k)\right). \quad (30)$$

step 3, parameter update using Eq. (17) and Eq. (18).

step 4, projection of unstable parameters: for $i = 1:n$, if $|\hat{\theta}_i(k)| > 1$, $\hat{\theta}_i(k) = \hat{\theta}_i(k-1)$.

step 5, *a posteriori* prediction error $\bar{e}(k)$ computation and state vector update: for $i = 1:n$

$$\bar{x}_i(k) = \left[2(\alpha-\beta)\hat{\theta}_i(k), \beta^2-\alpha^2\right] Z_i(k) + \bar{x}_{i-1}(k), \quad (31)$$

$$Z_i(k+1) = \left[\begin{array}{c|c} 2\alpha\hat{\theta}_i(k) & -\alpha^2 \\ \hline 1 & 0 \end{array}\right] Z_i(k) + \left[\begin{array}{c} 1 \\ \hline 0 \end{array}\right] \bar{x}_{i-1}(k), \quad (32)$$

with $\bar{x}_o(k) = z(k)$ and $\bar{e}(k) = \bar{x}_n(k)$.

$$W_i(\gamma,k+1) = \left[\begin{array}{c|c} 2\gamma\hat{\theta}_i(k) & -\gamma^2 \\ \hline 1 & 0 \end{array}\right] W_i(\gamma,k) + \left[\begin{array}{c} 1 \\ \hline 0 \end{array}\right] \bar{e}(k), \quad (33)$$

for $\gamma = \alpha,\beta$.

step 6, forgetting factor and notch filter shape coefficient update: replace α by $\alpha_{end} - [\alpha_{end} - \alpha]\alpha_{rate}$, and

$$\lambda(k+1) = \lambda_{end} - [\lambda_{end} - \lambda(k)]\lambda_{rate}. \quad (34)$$

Remark: (1) The above algorithm does not involve any sine or cosine functions, but instead performs one additional simple step to assure the stability of the filter. (2) The *a posteriori* information is applied as in [18], to improve the estimation precision. (3) As long as the initial parameter guesses are not too far away from the true values, the estimation is unbiased even under the presence of noise [18].

5 SIMULATION RESULT

The proposed adaptive compensator for multiple narrow-band disturbance rejection was implemented in the HDD benchmark simulation tool [12]. The baseline control system is as shown in Section 2. All common disturbances in HDD, including the torque disturbance, the disk flutter disturbance, the repeatable runout (RRO), and the measurement noise, are added in the simulation. The sampling time, the spindle rotation speed, and the track density are respectively 3.788×10^{-5} sec, 7200 rpm, and 100k Tracks Per Inch (TPI). The multiple narrow-band disturbance in NRRO was modeled as the sum of several sinusoidal signals [1, 2], and injected at the input to the plant with center frequencies 500 Hz and 1200 Hz.

Figure 7 shows the time trace of the position error signal without compensation. It is observed that the peak values of PES exceeded the standard PES upper bound of 15% Track Pitch (TP). The dotted line in Fig. 9 presents the spectrum of the PES without compensation. We can see that the PES had strong energy components at 500 Hz and 1200 Hz. Without compensation, the Track Mis-Registration (TMR), defined as 3 times the standard deviation of the PES, was 21.87% TP.

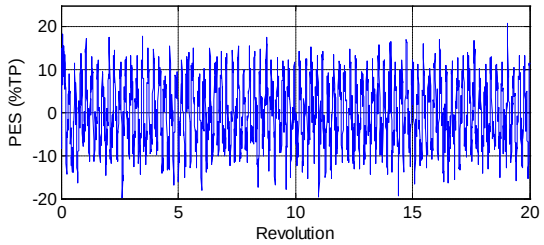

Figure 7. Time trace of the position error signal without compensation.

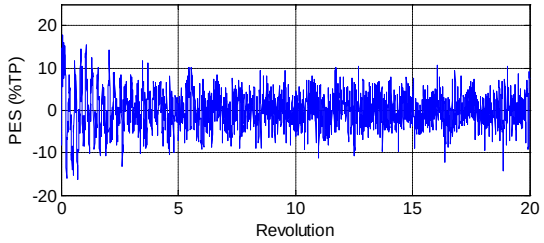

Figure 8. Time trace of the position error signal with compensation.

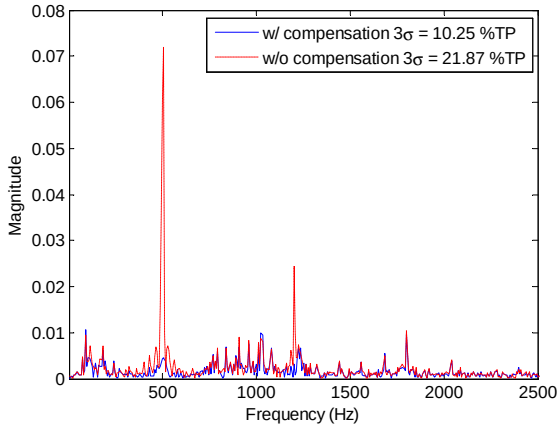

Figure 9. Spectra of the position error signals with and without the compensator.

With the same baseline controllers, the proposed add-on compensation scheme was applied to improve servo performance. The low-pass filter in Fig. 1 was designed using *MATLAB's Filter Design Toolbox*, to have a cut-off frequency of 2000 Hz. The parameter adaptation was initialized at $\hat{\theta}_i(0) = \cos(2\pi\Omega_i^o T_s)$, where $\Omega_1^o = 100$ Hz and $\Omega_2^o = 1000$ Hz, in view of the fact that the multiple narrow-band disturbance of interest lies between 300 Hz and 2000 Hz. Figure 10 shows the online identification of the parameters $\hat{\theta}_1$ and $\hat{\theta}_2$. Figure 11 shows the equivalent online frequency estimation, via the transformation $\hat{\Omega}_1 = \cos^{-1}(\hat{\theta}_1)/(2\pi T_s)$ and $\hat{\Omega}_2 = \cos^{-1}(\hat{\theta}_2)/(2\pi T_s)$. It is observed that the parameters converged to their true values within one revolution, i.e., 0.00833 sec.

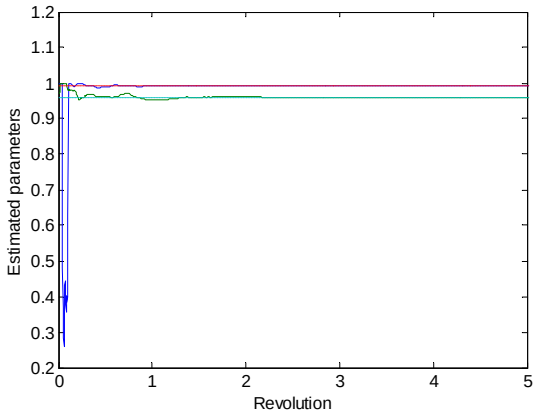

Figure 10. Online parameter estimation of the two narrow-band signals.

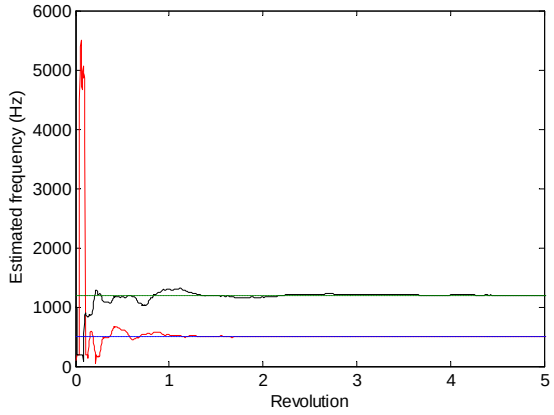

Figure 11. Equivalent frequency identification of the two narrow-band signals.

Recall the stability condition at the end of section 3, that $\hat{\Omega}_i(k)$ should be lower than the DOB stability threshold 3200 Hz. Correspondingly, $\hat{\theta}_i(k)$ should be larger than $\cos(2\pi \times 3200 T_S)$ for implementation. Once the estimated parameters fell into this region, the adaptive DOB was constructed to reject the multiple narrow-band disturbance.

Notice that the proposed Q-filter is given by

$$Q\left(z^{-1}\right) = \sum_{i=1}^{n} \frac{2\left(1-\alpha_i\right)\theta_i + \left(\alpha_i^2 - 1\right) z^{-1}}{1 - 2\alpha_i \theta_i z^{-1} + \alpha_i^2 z^{-2}}. \qquad (35)$$

In the simulation example, $n = 2$ and $\alpha_1 = \alpha_2 = 0.998$. To generate the compensation signal $c(k) = Q\left(z^{-1}\right)\hat{d}(k)$ at each iteration, Eq. (35) was realized by, in the state space form,

$$S_i(k+1) = \left[\begin{array}{c|c} 2\alpha\theta_i & -\alpha^2 \\ \hline 1 & 0 \end{array}\right] S_i(k) + \left[\begin{array}{c} 1 \\ \hline 0 \end{array}\right] \hat{d}(k) \tag{36}$$

$$c_i(k) = (1-\alpha)\left\{\left[4\alpha\theta_i^2 - 1 - \alpha, -2\alpha^2\theta_i\right] S_i(k) + 2\theta_i \hat{d}(k)\right\} \tag{37}$$

with θ_i replaced by its latest stable estimate $\hat{\theta}_i(k)$, and $c(k) = Q\left(z^{-1}\right)\hat{d}(k) = \sum_{i=1}^{n} c_i(k)$.

Figure 8 shows the resulting PES time trace. It is seen that after a transient response of about 1 revolution, the PES was reduced to within 10% TP. In the frequency domain, we observe from Fig. 9, that the strong energy components at 500 Hz and 1200 Hz were greatly attenuated, while the spectrum of the PES at other frequencies was almost identical to that without compensation. The TMR was reduced to 10.25% TP, implying a 53.13% improvement.

6 CONCLUSION

In this paper, an adaptive control scheme was proposed for rejecting multiple narrow-band disturbances in HDD track following. It consists of an adaptive notch filter to estimate the frequencies of the disturbances and a disturbance observer with a multiple band-pass filter tuned for the estimated frequencies. Simulation results on a realistic open-source HDD benchmark problem showed that the proposed algorithm significantly reduced the PES and the TMR. The proposed method is suitable in control systems that demand heavy disturbance attenuation at several frequencies.

ACKNOWLEDGMENT

This work was supported by the Computer Mechanics Laboratory (CML) in the Department of Mechanical Engineering, University of California at Berkeley. The authors gratefully acknowledge Dr. Qixing Zheng's useful discussions.

REFERENCES

[1] Guo, L., and Chen, Y., 2000. "Disk flutter and its impact on hdd servo performance". In Proceedings of 2000 Asia-Pacific Magnetic Recording Conference, pp. TA2/1–TA2/2.

[2] Ehrlich, R., and Curran, D., 1999. "Major HDD TMR sources and projected scaling with tpi". *IEEE Transactions on Magnetics,* **35**(2), pp. 885–891.

[3] McAllister, J., 1996. "The effect of disk platter resonances on track misregistration in 3.5 inch disk drives". *IEEE Transactions on Magnetics,* **32**(3), May, pp. 1762–1766.

[4] Zheng, Q., and Tomizuka, M., 2007. "Compensation of dominant frequency components of nonrepeatable disturbance in hard disk drives". *IEEE Transactions on Magnetics,* **43**(9), pp. 3756–3762.

[5] Zheng, Q., and Tomizuka, M., 2008. "A disturbance observer approach to detecting and rejecting narrow-band disturbances in hard disk drives". In Proceedings of 2008 IEEE International Workshop on Advanced Motion Control, pp. 254–259.

[6] Zheng, Q., and Tomizuka, M., 2006. "Compensation of dominant frequency component of Non-Repeatable runout in hard disk drives". In Proceedings of 2006 Asia-Pacific Magnetic Recording Conference, pp. 1–2.

[7] Kim, Y., Kang, C., and Tomizuka, M., 2005. "Adaptive and optimal rejection of non-repeatable disturbance in hard disk drives". In Proceedings of 2005 IEEE/ASME International Conference on Advanced Intelligent Mechatronics, Vol. 1, pp. 1–6.

[8] Landau, I. D., Constantinescu, A., and Rey, D., 2005. "Adaptive narrow band disturbance rejection applied to an active suspension–an internal model principle approach". *Automatica,* **41**(4), pp. 563–574.

[9] Nehorai, A., 1985. "A minimal parameter adaptive notch filter with constrained poles and zeros". *IEEE Transactions on Acoustics, Speech and Signal Processing,* **33**(4), Aug., pp. 983–996.

[10] Chen, B.-S., Yang, T.-Y., and Lin, B.-H., 1992. "Adaptive notch filter by direct frequency estimation". *Signal Processing,* **27**(2), pp. 161 – 176.

[11] Li, G., 1997. "A stable and efficient adaptive notch filter for direct frequency estimation". *IEEE Transactions on Signal Processing,* **45**(8), Aug., pp. 2001–2009.

[12] IEEJ, Technical Commitee for Novel Nanoscale Servo Control, 2007. NSS benchmark problem of hard disk drive systems. http://mizugaki.iis.u-tokyo.ac.jp/nss/.

[13] Ohnishi, K., 1993. "Robust motion control by disturbance observer". *Journal of the Robotics Society of Japan,* **11**(4), pp. 486–493.

[14] Tomizuka, M., 1987. "Zero phase error tracking algorithm for digital control". *Journal of Dynamic Systems, Measurement, and Control,* **109**(1), pp. 65–68.

[15] Kempf, C., and Kobayashi, S., 1996. "Discrete-time disturbance observer design for systems with time delay". In Proceedings of 4th International Workshop on Advanced Motion Control, Vol. 1, pp. 332–337.

[16] Kempf, C., and Kobayashi, S., 1999. "Disturbance observer and feedforward design for a high-speed direct-drive positioning table". *IEEE Transactions on Control Systems Technology,* **7**(5), pp. 513–526.

[17] Oppenheim, A., Schafer, R., and Buck, J., 1989. *Discrete-time signal processing*. Prentice hall Englewood Cliffs, NJ.

[18] Ljung, L., 1999. *System Identification: Theory for the User*, 2 ed. Prentice Hall PTR.